Journal of Computational Mathematics
Vol.xx, No.x, 2025, 1–13.

http://www.global-sci.org/jcm
doi:10.4208/jcm.2506-m2025-0066

A SIMPLE ERROR ESTIMATE OF DISCONTINUOUS GALERKIN METHODS FOR ELLIPTIC EQUATIONS WITH LOW REGULARITY*

Kaifang Liu
College of Mathematical Science, Yangzhou University, Yangzhou 225002, China
Email: kliu@yzu.edu.cn

Abstract

In this work, we develop a low-regularity error analysis for the interior-penalty discontinuous Galerkin (IPDG) method, incorporating numerical fluxes originally proposed by Brezzi *et al.* [Numer. Methods Partial Differential Equations, 16 (2000)]. Our analysis specifically addresses elliptic problems with solutions residing in the low-regularity space H^s, where $0 \leq s < 1/2$. Notably, our error estimates hold under two critical settings: discontinuous coefficients and general Lipschitz domains, precisely capturing the essential features of practical applications. We establish error estimates in the energy norm and the L^2-norm, providing a complete theoretical framework for the IPDG method in low-regularity limitation. To systematically verify the theoretical results, we conduct some numerical experiments incorporating precision-controlled parameters that directly correspond to the analytical model's constraints.

Mathematics subject classification: 65N12, 65N15.
Key words: Discontinuous Galerkin, Second-order elliptic equations, Minimal regularity, Lifting operator.

1. Introduction

Let Ω be a Lipschitz domain in $\mathbb{R}^d$ $(d = 2, 3)$ with boundary Γ and suppose the domain is partitioned into M connected Lipschitz subdomains $\Omega_i, i = 1, \ldots, M$. The domain Ω and subdomains Ω_i can be convex or concave. The second-order elliptic problem with homogeneous Dirichlet boundary condition

$$-\nabla \cdot A\nabla u = f \quad \text{in } \Omega, \tag{1.1}$$

$$u = 0 \qquad \text{on } \Gamma, \tag{1.2}$$

where $f \in L^2(\Omega)$ is the source term and A is a symmetric positive definite matrix-valued function on Ω and bounded below and above uniformly, i.e. there exist two positive numbers A_0 and A_1 such that

$$A_0\xi^\top\xi \leq \xi^\top A\xi \leq A_1\xi^\top\xi, \quad \forall\, \xi \in \mathbb{R}^d,$$

where $\xi \in \mathbb{R}^d$ is a column vector and $\xi^\top$ means the transpose of ξ. For simplicity, we always assume that A is piecewise in $W^{1,\infty}(\Omega_i), i = 1, \ldots, M$.

Low-regularity elliptic problems, as considered in our setting, serve as prototype models for various applications, including acoustics [13], material science [14], and fluid dynamics [23].

* Received March 2, 2025 / Revised version received May 19, 2025 / Accepted June 23, 2025 / Published online November 26, 2025 /

For example, in photonic crystals, the low regularity of electromagnetic fields and Lagrange multiplier lies on the interface of two different materials [3]. Low regularity often arises from discontinuities in the coefficients of governing equations, non-smooth domain boundaries, or singularities in the solution itself. In this paper, the low regularity primarily stems from discontinuous coefficients and non-smooth domain boundaries. For an introduction to this topic in mathematical view, see [11].

There are quite a lot of papers dealing with discontinuous Galerkin (DG) discretization of elliptic problems under standard regularity assumptions with solutions in $H^m(\Omega), m \geq 2$ or $H^{1+s}(\Omega), s > 1/2$; see, e.g. [2, 5, 6, 15, 20] and references therein. An analysis of DG method with weak solutions in $W^{2,p}(\Omega), p \in (1, 2]$ can be found in [19, 24]. The low regularity of solutions brings great challenge for deriving a priori error estimate of the DG methods. The main difficulty of the DG discretization is that the numerical fluxes across mesh faces are not well-defined in the sense of standard trace theorem, which directly makes the consistency of DG discretization unclear. Gudi [12] introduced a new framework of error analysis under low regularity requirements avoiding the above issue. Recently, Ern and Guermond [9] proposed an error analysis of nonconforming finite element methods (FEMs), where a weak meaning of normal trace on mesh faces is defined for low regularity functions.

In this paper, we will present a simple a priori estimate of the IPDG method with the numerical fluxes introduced by Brezzi *et al.* [5] under minimal smoothness requirements. First, with the Brezzi flux in DG formulation, the bilinear form is well-defined for all weak solutions in $H^1(\Omega)$. Second, by using quasi-interpolation operators that satisfy commutative diagram and employing that $A\nabla u \in H(\mathrm{div}, \Omega)$, a consistency result (or residual equation) is established. Third, duality argument is carried out by using the regularity result in [3, Theorem 3.1].

The weak formulation of (1.1) states: Find $u \in V := H_0^1(\Omega)$ such that

$$a(u, v) := (A\nabla u, \nabla v) = (f, v), \quad \forall\, v \in V. \tag{1.3}$$

We can see from the weak formulation (1.3), that

$$A\nabla u \in H(\mathrm{div}, \Omega) = \{\boldsymbol{v} \in L^2(\Omega)^d \,:\, \nabla \cdot \boldsymbol{v} \in L^2(\Omega)\}.$$

In the following, we will use the standard Sobolev notation [1]. For a generic bounded domain $D \subset \mathbb{R}^d$, we denote by $W^{m,p}(D)$ the usual Sobolev space of order $m \in \mathbb{N}$ with norms $\|\cdot\|_{m,p,D}$, and write $H^m(D) = W^{m,2}(D)$ with norm $\|\cdot\|_{m,D}$. The fractional Sobolev spaces $H^s(D)$ (respectively, $H_0^s(D)$), $s \in (m, m+1)$ are defined by real interpolation between $H^m(D)$ and $H^{m+1}(D)$ (respectively, $H_0^m(D)$ and $H_0^{m+1}(D)$) (see [4,22]). We denote by $(\cdot\,,\cdot)_D$ the standard inner product in $L^2(D)^d$.

The paper is organized as follows. In Section 2, we introduce some preliminaries and in Section 3, we set the IPDG method with the numerical flux introduced by Brezzi *et al.* [5]. We present the main error estimates for low regularity solution in Section 4. In Section 5, we conduct numerical experiments to validate theoretical results, and in Section 6, we give a summation of the work.

2. Preliminaries

Let $\mathcal{T}_h$ be a shape regular partition of the domain Ω (triangle for $d = 2$ and tetrahedral for $d = 3$) without hanging nodes such that A is locally in $W^{1,\infty}$ within each element $K \in \mathcal{T}_h$. Denote by $\mathcal{F}_h$ the union of interior faces $\mathcal{F}_h^I$ and boundary faces $\mathcal{F}_h^B$. Define h_K to be the

diameter of $K \in \mathcal{T}_h$. For an integer $\ell \geq 0$, let $\mathbb{P}_\ell(K)$ be the space of polynomial of total degree ℓ in $K \in \mathcal{T}_h$. Denote by $\boldsymbol{v}$ and v smooth vector- or scalar-valued functions and assume $F \in \mathcal{F}_h^I$ be shared by two elements K^+ and K^-. The normal jump across F is defined by $[\![v]\!]_N = v^+\boldsymbol{n}^+ + v^-\boldsymbol{n}^-$, where $v^\pm = v|_{K^\pm}$ and $\boldsymbol{n}^\pm$ represent the unit normal vector on F pointing to $K^\mp$. We also denote the average of scalar-valued function v by $\{\!\{v\}\!\} = (v^+ + v^-)/2$, and similarly for vector-valued function $\{\!\{\boldsymbol{v}\}\!\} = (\boldsymbol{v}^+ + \boldsymbol{v}^-)/2$. For the boundary edge $F \in \mathcal{F}_h^B$, we set $[\![v]\!]_N = v\boldsymbol{n}$, $\{\!\{v\}\!\} = v$ and $\{\!\{\boldsymbol{v}\}\!\} = \boldsymbol{v}$.

2.1. Finite element spaces

Define the discontinuous Galerkin finite element space

$$V_h := \big\{v \in L^2(\Omega) \,:\, v_{|K} \in \mathbb{P}_\ell(K)^d,\ \forall\, K \in \mathcal{T}_h\big\}, \tag{2.1}$$

and the H^1-conforming subspace of V_h as follows:

$$V_h^{\mathrm{c}} = V_h \cap H^1(\Omega), \quad V_{h0}^{\mathrm{c}} = V_h \cap V.$$

Moreover, we introduce the broken $H(\mathrm{div})$ finite element space

$$\boldsymbol{W}_h := \big\{\boldsymbol{v} \in L^2(\Omega)^d :\ \boldsymbol{v}_{|K} \in D_\ell(K),\ \forall\, K \in \mathcal{T}_h\big\}, \tag{2.2}$$

where

$$D_\ell(K) = (\mathbb{P}_{\ell-1})^d \oplus (\widetilde{\mathbb{P}}_{\ell-1})^d\boldsymbol{x},$$

and $\widetilde{\mathbb{P}}_{\ell-1}$ denotes the homogeneous polynomials of degree ℓ (see [17, Section 5.4]). Let Z_h denote the finite element space [17, Section 5.7]

$$Z_h := \big\{v \in L^2(\Omega) :\ v_{|K} \in \mathbb{P}_{\ell-1}(K),\ \forall\, K \in \mathcal{T}_h\big\}. \tag{2.3}$$

We denote by $\boldsymbol{W}_h^{\mathrm{c}} = \boldsymbol{W}_h \cap H(\mathrm{div}, \Omega)$ the $H(\mathrm{div})$-conforming subspace. It is well known that $\boldsymbol{W}_h$ and Z_h satisfy local discrete de Rham complex, which will be used in the error analysis.

2.2. Lifting operator

The local lifting operator $\mathcal{R}_F :\ L^2(F)^d \to \boldsymbol{W}_h$ on a face $F \in \mathcal{F}_h$ is defined by

$$\int_\Omega \mathcal{R}_F(\lambda) \cdot \boldsymbol{v}\,\mathrm{d}\boldsymbol{x} = \int_F \lambda \cdot \{\!\{\boldsymbol{v}\}\!\}\,\mathrm{d}s \tag{2.4}$$

for all $\lambda \in L^2(F)^d$ and $\boldsymbol{v} \in \boldsymbol{W}_h$. Since the operator is locally defined, the support of lifting function $\mathcal{R}_F(\lambda)$ is the union of elements adjacent to F. The global lifting operator $\mathcal{R} : L^2(\mathcal{F}_h)^d \to \boldsymbol{W}_h$ has the summation form $\mathcal{R} = \sum_{F\in\mathcal{F}_h} \mathcal{R}_F$.

We endow $V(h) := V_h + V$ with the norm

$$\|v\|_{V(h)}^2 := \big\|A^{\frac{1}{2}}\nabla_h v\big\|_{0,\Omega}^2 + \sum_{F\in\mathcal{F}_h} \big\|A^{\frac{1}{2}}\mathcal{R}_F([\![v]\!]_N)\big\|_{0,\Omega}^2, \tag{2.5}$$

where ∇_h denotes the broken gradient over elements. Moreover, the following stability result will be useful.

Lemma 2.1 ([5, Lemma 2]). *There exist two positive constants C_1 and C_2, independent of h such that*

$$C_1\big\|h_F^{-\frac{1}{2}}[\![v]\!]_N\big\|_{0,F} \le \|\mathcal{R}_F([\![v]\!]_N)\|_{0,\Omega} \le C_2\big\|h_F^{-\frac{1}{2}}[\![v]\!]_N\big\|_{0,F} \tag{2.6}$$

for all $v \in V_h$ and for all $F \in \mathcal{F}_h$.

By using the stability of lifting operator $\mathcal{R}_F$ in (2.6), we obtain

Lemma 2.2 ([15, Theorem 2.2]). *Given a regular partition $\mathcal{T}_h$ of Ω, there exists an H^1-conforming projection $\Pi_h^c : V_h \to V_h^c$ such that*

$$h_K^{-2}\big\|v - \Pi_h^c v\big\|_{0,K}^2 + \big\|\nabla\big(v - \Pi_h^c v\big)\big\|_{0,K}^2 \le c \sum_{F\in\partial K} \|\mathcal{R}_F([\![v]\!]_N)\|_{0,\Omega}^2$$

for all $v \in V_h$. Here, $c > 0$ is independent of the mesh size.

3. Interior Penalty Discontinuous Galerkin Method

The discontinuous Galerkin finite element method states: Find $u_h \in V_h$ such that

$$a_h(u_h, v) = (f, v), \quad \forall\, v \in V_h, \tag{3.1}$$

where

$$\begin{aligned} a_h(u,v) = {} & (A\nabla_h u, \nabla_h v) - \big(\mathcal{R}([\![u]\!]_N), A\nabla_h v\big) \\ & - \big(\mathcal{R}([\![v]\!]_N), A\nabla_h u\big) + \sum_{F\in\mathcal{F}_h} \alpha_F\big(A\mathcal{R}_F([\![u]\!]_N), \mathcal{R}_F([\![v]\!]_N)\big). \end{aligned} \tag{3.2}$$

Remark 3.1. Since $\nabla_h v \in \boldsymbol{W}_h$ for all $v \in V_h$, if A is piecewise constant it holds from (2.4) that for any $u, v \in V_h$,

$$\begin{aligned} a_h(u,v) = {} & (A\nabla_h u, \nabla_h v) - \int_{\mathcal{F}_h} [\![u]\!]_N \cdot \{\!\{A\nabla_h v\}\!\}\,\mathrm{d}s \\ & - \int_{\mathcal{F}_h} [\![v]\!]_N \cdot \{\!\{A\nabla_h u\}\!\}\,\mathrm{d}s + \sum_{F\in\mathcal{F}_h} \alpha_F\big(A\mathcal{R}_F([\![u]\!]_N), \mathcal{R}_F([\![v]\!]_N)\big). \end{aligned} \tag{3.3}$$

Remark 3.2. If we introduce a parameter ϵ into the bilinear form (3.2)

$$\begin{aligned} a_h(u,v) = {} & (A\nabla_h u, \nabla_h v) + \epsilon\big(\mathcal{R}([\![u]\!]_N), A\nabla_h v\big) \\ & - \big(\mathcal{R}([\![v]\!]_N), A\nabla_h u\big) + \sum_{F\in\mathcal{F}_h} \alpha_F\big(A\mathcal{R}_F([\![u]\!]_N), \mathcal{R}_F([\![v]\!]_N)\big), \end{aligned}$$

this modification results in symmetric, nonsymmetric, and incomplete IPDG methods for $\epsilon = -1, +1, 0$, respectively. For further details, see [20]. The analysis presented in this paper primarily focuses on the symmetric case, but it can be readily extended to the other two cases.

Remark 3.3. For the inhomogeneous boundary condition $u_{|\Gamma} = g \in L^2(\Gamma)$, the right-hand side of (3.1) will be

$$f_h(v) = (f, v) - \sum_{F\in\mathcal{F}_h^B} \big(\mathcal{R}_F(g\boldsymbol{n}_F), A\nabla_h v\big) + \sum_{F\in\mathcal{F}_h^B} \alpha_F\big(A\mathcal{R}_F(g\boldsymbol{n}_F), \mathcal{R}_F([\![v]\!]_N)\big).$$

Remark 3.4. The bilinear form $a_h : H^1(\Omega) \times H^1(\Omega) \to \mathbb{R}$ is well-defined, because for all $v \in H^1(\Omega), [\![v]\!]_N = 0$ on each $F \in \mathcal{F}_h^I$ and $[\![v]\!]_N \in L^2(F)$ on each $F \in \mathcal{F}_h^B$.

The well-posedness of the DG formulation (3.1) is a direct result of continuity and coercivity stated in the following, see, for example, [5,6] for a proof.

Lemma 3.1 (Continuity). *There exists a constant C independent of the mesh size, coefficient A such that*

$$|a_h(u,v)| \le C\|u\|_{V(h)}\|v\|_{V(h)}, \quad \forall\, u, v \in V(h).$$

Lemma 3.2 (Coercivity). *There exists a constant $\kappa > 0$ such that*

$$a_h(v,v) \ge \kappa \|v\|_{V(h)}^2, \quad \forall\, v \in V_h.$$

Here, $\kappa = 1/2$ for all $\alpha_F \ge 1/2 + 2n_K$ with $n_K = d+1$ being the number of faces of elements $K \in \mathcal{T}_h$.

4. Error Analysis

In this section, we present our main result in error estimates.

4.1. Error estimate in energy norm

Suppose $u \in V$ is the weak solution of (1.3). Define the residual operator and its norm

$$\mathfrak{R}(u,v) := a_h(u,v) - (f,v), \quad \mathfrak{R}(u) := \sup_{v \in V_h} \frac{\mathfrak{R}(u,v)}{\|v\|_{V(h)}}, \quad \forall\, v \in V_h. \tag{4.1}$$

It is worthy to note that $\mathfrak{R}(u,v) = a_h(u - u_h, v)$ for any $v \in V_h$ for the DG approximation $u_h \in V_h$.

Lemma 4.1 (Orthogonality). *Let $u \in V$ be the solution of (1.3). Then, $\mathfrak{R}(u,v) = 0$ for all $v \in V_{h0}^{\mathrm{c}}$.*

Proof. Since $u \in V$ and $v \in V_{h0}^{\mathrm{c}}, [\![u]\!]_N = [\![v]\!]_N = 0$ and

$$\mathfrak{R}(u,v) = a_h(u,v) - (f,v) = (A\nabla u, \nabla v) - (f,v).$$

Hence, by an integration by parts, we obtain $\mathfrak{R}(u,v) = 0$. □

Proposition 4.1 (Residual Equation). *Let $u \in V$ be the solution of (1.3). It holds that*

$$\mathfrak{R}(u,v) = \big(\varepsilon_1(u), \nabla_h v\big) + \big(\varepsilon_2(u), v\big) - \big(\mathcal{R}([\![v]\!]_N), \varepsilon_1(u)\big) \tag{4.2}$$

for all $v \in V_h$. Here, $\sigma(u) := A\nabla u$ and

$$\varepsilon_1(u) := \sigma(u) - \mathcal{J}_h^{\mathrm{d}}\sigma(u), \quad \varepsilon_2(u) := \nabla\cdot\sigma(u) - \mathcal{J}_h^{\mathrm{b}}\nabla\cdot\sigma(u),$$

where $\mathcal{J}_h^{\mathrm{d}}$ and $\mathcal{J}_h^{\mathrm{b}}$ are quasi-interpolations defined in [7].

Proof. For any $v \in V_h$, it is clear from $[\![u]\!]_N = 0$ that

$$\begin{aligned}\mathfrak{R}(u,v) &= \big(\sigma(u), \nabla_h v\big) - \big(\mathcal{R}([\![v]\!]_N), \sigma(u)\big) - (f, v)\\ &= \big(\sigma(u), \nabla_h v\big) - \big(\mathcal{R}([\![v]\!]_N), \sigma(u)\big) + \big(\nabla\cdot\sigma(u), v\big). \end{aligned} \tag{4.3}$$

By using the smoothed interpolation $\mathcal{J}_h^{\mathrm{d}} : H(\mathrm{div}, \Omega) \to \boldsymbol{W}_h^{\mathrm{c}}$, one arrives at

$$\big(\mathcal{R}([\![v]\!]_N), \sigma(u)\big) = \big(\mathcal{R}([\![v]\!]_N), \mathcal{J}_h^{\mathrm{d}}\sigma(u)\big) + \big(\mathcal{R}([\![v]\!]_N), \varepsilon_1(u)\big).$$

From the definition of $\mathcal{R}$, we infer that

$$\big(\mathcal{R}([\![v]\!]_N), \mathcal{J}_h^{\mathrm{d}}\sigma(u)\big) = \int_{\mathcal{F}_h} [\![v]\!]_N \cdot \big\{\!\big\{\mathcal{J}_h^{\mathrm{d}}\sigma(u)\big\}\!\big\}\,\mathrm{d}s = \big(\nabla\cdot\mathcal{J}_h^{\mathrm{d}}\sigma(u), v\big) + \big(\mathcal{J}_h^{\mathrm{d}}\sigma(u), \nabla_h v\big),$$

and obtain

$$\big(\mathcal{R}([\![v]\!]_N), \sigma(u)\big) = \big(\nabla\cdot\mathcal{J}_h^{\mathrm{d}}\sigma(u), v\big) + \big(\mathcal{J}_h^{\mathrm{d}}\sigma(u), \nabla_h v\big) + \big(\mathcal{R}([\![v]\!]_N), \varepsilon_1(u)\big).$$

Using the commuting diagram $\nabla\cdot\mathcal{J}_h^{\mathrm{d}}\sigma(u) = \mathcal{J}_h^{\mathrm{b}}\nabla\cdot\sigma(u)$ and substituting into (4.3) complete the proof. □

Proposition 4.2 (Residual Estimate). *Let $u \in V$ be the solution of* (1.3) *with $u \in H^{1+s}(\mathcal{T}_h)$, $0 \le s < 1/2$. It holds that*

$$\mathfrak{R}(u) \le C\left(\sum_{K\in\mathcal{T}_h} h_K^{2s}\|A\nabla u\|_{s,D_K}^2 + h_K^2\|\nabla\cdot A\nabla u\|_{0,D_K}^2\right)^{\frac{1}{2}}, \tag{4.4}$$

where the constant $C > 0$ is independent of the mesh size h and $D_K := \mathrm{int}(\cup_{K_i\cap K\neq\emptyset}\bar{K}_i)$ denotes the patch around the element K.

Proof. Let $v^\perp = v - \Pi_h^{\mathrm{c}} v \in V_h$ for all $v \in V_h$ and recall $\sigma(u) = A\nabla u$. It is clear that the residual equation (4.2) also holds for $\Pi_h^{\mathrm{c}} v \in V_{h0}^{\mathrm{c}}$. From Lemma 4.1, we know $\mathfrak{R}(u, \Pi_h^{\mathrm{c}} v) = 0$. From Proposition 4.1, one obtains

$$\begin{aligned}\mathfrak{R}(u,v) = \mathfrak{R}(u,v^\perp) &= \big(\varepsilon_1(u), \nabla v^\perp\big) + \big(\varepsilon_2(u), v^\perp\big) - \big(\mathcal{R}\big([\![v^\perp]\!]_N\big), \varepsilon_1(u)\big)\\ &\le \sum_{K\in\mathcal{T}_h} \|\varepsilon_1(u)\|_{0,K}\big(\|\nabla v^\perp\|_{0,K} + \big\|\mathcal{R}\big([\![v^\perp]\!]_N\big)\big\|_{0,K}\big) + \|\varepsilon_2(u)\|_{0,K}\|v^\perp\|_{0,K}. \end{aligned} \tag{4.5}$$

Thus, Lemma 2.2 leads to

$$\mathfrak{R}(u,v) \le C\left(\sum_{K\in\mathcal{T}_h} \|\varepsilon_1(u)\|_{0,K}^2 + h_K^2\|\varepsilon_2(u)\|_{0,K}^2\right)^{\frac{1}{2}}\left(\sum_{F\in\mathcal{T}_h} \|\mathcal{R}_F([\![v]\!]_N)\|_{0,\Omega}^2\right)^{\frac{1}{2}},$$

where the constant C could rely on the regularity of $\mathcal{T}_h$. The estimate (4.4) follows directly from the best quasi-approximation [8, Theorem 5.2]. □

Proposition 4.3 (Error Estimates). *Let $u \in V$ solve* (1.3) *with*

$$u \in H^{1+s}(\mathcal{T}_h), \quad 0 \le s < \frac{1}{2},$$

and let $u_h \in V_h$ solve (3.1). *Then, there exists a constant $C > 0$ independent of the mesh size h such that*

$$\|u - u_h\|_{V(h)} \le C\Big(\mathfrak{R}(u) + \inf_{v\in V_h} \|u - v\|_{V(h)}\Big), \tag{4.6}$$

$$\|u - u_h\|_{V(h)} \le C\left(\sum_{K\in\mathcal{T}_h} h_K^{2s}\|A\nabla u\|_{s,D_K}^2 + h_K^2\|\nabla\cdot A\nabla u\|_{0,D_K}^2\right)^{\frac{1}{2}}. \tag{4.7}$$

Proof. By using the continuity and coercivity of a_h in Lemmas 3.1 and 3.2, respectively, we have for any $v \in V_h$,

$$\begin{aligned}\kappa\|u_h - v\|_{V(h)}^2 &\le a_h(u_h - v, u_h - v)\\ &\le a_h(u_h - u, u_h - v) + a_h(u - v, u_h - v)\\ &= -\mathfrak{R}(u, u_h - v) + a_h(u - v, u_h - v)\\ &\le C\big(\mathfrak{R}(u) + \|u - v\|_{V(h)}\big)\|u_h - v\|_{V(h)}.\end{aligned}$$

Therefore, the estimate (4.6) follows directly from

$$\begin{aligned}&\|u - u_h\|_{V(h)} \le \|u - v\|_{V(h)} + \|u_h - v\|_{V(h)},\\ &\|u_h - v\|_{V(h)} \le \frac{C}{\kappa}\big(\mathfrak{R}(u) + \|u - v\|_{V(h)}\big), \quad \forall\, v \in V_h.\end{aligned}$$

The estimate (4.7) results from (4.4) and the best approximation

$$\inf_{v\in V_h} \|u - v\|_{V(h)} \le C\left(\sum_{K\in\mathcal{T}_h} h_K^{2\min\{s,\ell\}}\|A\nabla u\|_{s,D_K}^2\right)^{\frac{1}{2}}. \tag{4.8}$$

Note that (4.8) is from Clément [17, Section 5.6.1] or Scott-Zhang [4,21] interpolation operators. The proof is complete. □

4.2. Duality argument

In this section, we will present the error estimate in L^2-norm via the standard duality argument. Suppose $u \in V$ solves (1.3) and $u_h \in V_h$ solves (3.1). We consider the following dual problem:

$$\begin{aligned}-\nabla\cdot A\nabla w &= u - u_h \qquad &&\text{in } \Omega,\\ w &= 0 &&\text{on } \Gamma,\end{aligned} \tag{4.9}$$

for which there always exists an $r \in (0, 1/2]$ such that the regularity estimate holds true [3, Theorem 3.1]

$$\|w\|_{1+r,\Omega} \le C\|u - u_h\|_{0,\Omega}. \tag{4.10}$$

Let w_h be the DG solution of (4.9). Then, (4.7) and (4.10) imply that

$$\|w - w_h\|_{V(h)} \le Ch^r(\|w\|_{1+r,\Omega} + \|u - u_h\|_{0,\Omega}) \le Ch^r\|u - u_h\|_{0,\Omega}, \tag{4.11}$$

where the constant $C > 0$ is independent of the mesh size h.

Proposition 4.4 (Error Estimate in L^2-norm). *Let $u \in V$ be the unique solution of (1.3) with $u \in H^{1+s}(\mathcal{T}_h), s \geq 0$ and let $u_h \in V_h$ solve (3.1). Let $r > 0$ be the regularity exponent in (4.10). There exists a constant $C > 0$ independent of the mesh size such that*

$$\|u - u_h\|_{0,\Omega} \leq Ch^r[\|u - u_h\|_{V(h)} + \mathfrak{R}(u)]. \tag{4.12}$$

Proof. Let w, w_h be the solutions of the dual problem and the corresponding DG method, respectively. Then, they satisfy

$$a_h(w, u) = (u - u_h, u), \quad a_h(w_h, u_h) = (u - u_h, u_h).$$

Recalling the definition of the residual (4.1), together with the above two identities, we derive

$$\begin{aligned}
&(u - u_h, u - u_h)\\
&= a_h(w, u) - a_h(w_h, u_h)\\
&= a_h(w - w_h, u - u_h) + a_h(w - w_h, u_h) + a_h(w_h, u - u_h)\\
&= a_h(w - w_h, u - u_h) + \mathfrak{R}(w, u_h) + \mathfrak{R}(u, w_h),
\end{aligned}$$

where we have used the symmetry of a_h. The remainder is to estimate the three terms above. First, from the continuity of $a_h(\cdot\,,\cdot)$ in Lemma 3.1 and the estimate (4.11), we have

$$a_h(w - w_h, u - u_h) \leq \|w - w_h\|_{V(h)}\|u - u_h\|_{V(h)} \leq Ch^r\|u - u_h\|_{V(h)}\|u - u_h\|_{0,\Omega}.$$

Second, from the proofs of Propositions 4.1 and 4.2, we know that

$$\begin{aligned}
\mathfrak{R}(u, w_h) &\leq C\mathfrak{R}(u)\left(\sum_{F\in\mathcal{T}_h}\|\mathcal{R}_F([\![w_h]\!]_N)\|_{0,\Omega}^2\right)^{\frac{1}{2}}\\
&\leq C\mathfrak{R}(u)\|w - w_h\|_{V(h)} \leq Ch^r\mathfrak{R}(u)\|u - u_h\|_{0,\Omega},
\end{aligned}$$

where we have used (4.11) in the last step. Third, from the estimate (4.4) and (4.10), we obtain

$$\begin{aligned}
\mathfrak{R}(w, u_h) &\leq C\mathfrak{R}(w)\left(\sum_{F\in\mathcal{T}_h}\|\mathcal{R}_F([\![u_h]\!]_N)\|_{0,\Omega}^2\right)^{\frac{1}{2}}\\
&\leq C\mathfrak{R}(w)\|u - u_h\|_{V(h)} \leq Ch^r\|u - u_h\|_{V(h)}\|u - u_h\|_{0,\Omega}.
\end{aligned}$$

Thus, the estimate (4.12) follows easily from the above three inequalities. □

5. Numerical Results

In this section, we present a series of numerical experiments to validate the theoretical predictions regarding the penalty parameter and convergence behavior. Throughout our simulations, we set the polynomial degree as $k \geq 1$ and adopt $[\mathbb{P}_{k-1}(K)]^2$ for the image of the lifting operator $\mathcal{R}_F$ across all elements $K \in \mathcal{T}_h$ to maintain consistency and simplicity. Furthermore, all computational domains are partitioned using the GMSH software [10], ensuring high-quality mesh generation for our numerical framework.

Example 5.1. Consider Poisson equation defined on $[0,1]^2$ with the exact solution

$$u = \sin(\pi x)\sin(\pi y).$$

The boundary condition and the source term $f(x,y)$ are derived accordingly.

We present numerical results in Tables 5.1 and 5.2 for the penalty parameters $\alpha_F = 3$ and $\alpha_F = 2$, respectively, to investigate the performance of the proposed IPDG method (3.1). From the tabulated data, we observe that the discrete solutions converge to the analytical ones at the theoretically optimal rate. Furthermore, our experiments reveal that the stability of the IPDG formulation can be easily achieved with relatively modest penalty parameter values, compared to conventional approaches without using lifting operators, where the penalty parameter depends on the geometry of physical element and degree of polynomials. Notably, the lower bound of the penalty parameter is governed by the number of element edges (faces in 3d, correspondingly), a property that aligns with the known conclusion and ensures the robustness of the method across different mesh configurations.

Table 5.1: Example 5.1. Convergent history of DG ($k = 1, \alpha_F = 3$).

$1/h$	$\|u - u_h\|_{V(h)}$	Rate	$\|u - u_h\|_{L^2(\Omega)}$	Rate
4	6.3630e-01		2.5167e-02	
8	3.2352e-01	0.9758	6.5307e-03	1.9462
16	1.6236e-01	0.9946	1.6461e-03	1.9881
32	8.1254e-02	0.9987	4.1234e-04	1.9972
64	4.0635e-02	0.9997	1.0313e-04	1.9993

Table 5.2: Example 5.1. Convergent history of DG ($k = 1, \alpha_F = 2$).

$1/h$	$\|u - u_h\|_{V(h)}$	Rate	$\|u - u_h\|_{L^2(\Omega)}$	Rate
4	3.5710e+00		1.5727e-01	
8	1.4185e+01	-1.9900	3.1344e-01	-0.9949
16	1.7344e+01	-0.2901	1.9163e-01	0.7099
32	3.8625e+00	2.1668	2.1337e-02	3.1669
64	7.9022e+00	-1.0327	2.1827e-02	-0.0328

Example 5.2. Consider Poisson equation defined on the slit domain $[-1,1]^2 \setminus [0,1] \times \{0\}$. Let the exact solution

$$u = r^{\frac{1}{2}} \sin\left(\frac{\theta}{2}\right),$$

where u is expressed in polar system, i.e. $r = \sqrt{x^2 + y^2}$. The boundary condition and the source term $f(x,y)$ are obtained accordingly. It is known that $u \in H^{1/2-\epsilon}(\Omega)$ for any small positive number ϵ.

Numerical results corresponding to $k = 1$ and $k = 2$ are presented in Tables 5.3 and 5.4, respectively. These results exhibit excellent agreement with our theoretical predictions, demonstrating that convergence rate of error in L^2-norm error is precisely twice in the energy norm. We guess it is because the analytic solution has exactly the same regularity of duality problem, see [11].

Table 5.3: Example 5.2. Convergent history of DG ($k = 1, \alpha_F = 3$).

$1/h$	$\|u - u_h\|_{V(h)}$	Rate	$\|u - u_h\|_{L^2(\Omega)}$	Rate
4	2.9307e-01		4.2510e-02	
8	2.1311e-01	0.4596	2.1268e-02	0.9991
16	1.5284e-01	0.4795	1.0632e-02	1.0002
32	1.0885e-01	0.4897	5.3158e-03	1.0001
64	7.7246e-02	0.4948	2.6580e-03	0.9999

Table 5.4: Example 5.2. Convergent history of DG ($k = 2, \alpha_F = 3$).

$1/h$	$\|u - u_h\|_{V(h)}$	Rate	$\|u - u_h\|_{L^2(\Omega)}$	Rate
4	1.3572e-01		1.0365e-02	
8	9.6181e-02	0.4969	5.0966e-03	1.0242
16	6.8075e-02	0.4986	2.5265e-03	1.0124
32	4.8159e-02	0.4993	1.2577e-03	1.0063
64	3.4061e-02	0.4997	6.2748e-04	1.0032

Example 5.3. Consider the problem (1.1), (1.2) defined on the unit square domain $\Omega = [-1, 1]^2$ with discontinuous coefficient A. We separate Ω into four quadrants, and the coefficient $A = A_1$ in the first and third quadrants and $A = A_2$ in the second and fourth quadrants. Set the exact solution to be (in this case $f = 0$)

$$u(r, \theta) = r^\gamma v(\theta),$$

where $\gamma \in (0, 1]$ and

$$v(\theta) = \begin{cases} \cos\left(\left(\frac{\pi}{2} - \sigma\right)\gamma\right)\cos\left(\left(\theta - \frac{\pi}{2} + \rho\right)\gamma\right), & 0 \le \theta \le \frac{\pi}{2}, \\ \cos(\rho\gamma)\cos\big((\theta - \pi + \sigma)\gamma\big), & \frac{\pi}{2} \le \theta \le \pi, \\ \cos(\sigma\gamma)\cos\big((\theta - \pi - \rho)\gamma\big), & \pi \le \theta \le \frac{3\pi}{2}, \\ \cos\left(\left(\frac{\pi}{2} - \rho\right)\gamma\right)\cos\left(\left(\theta - \frac{3\pi}{2} - \sigma\right)\gamma\right), & \frac{3\pi}{2} \le \theta \le 2\pi. \end{cases}$$

The parameters γ, ρ, σ satisfy the following nonlinear relations:

$$\begin{aligned} & R := \frac{A_1}{A_2} = -\tan\left(\left(\frac{\pi}{2} - \sigma\right)\gamma\right)\cot(\rho\gamma), \\ & \frac{1}{R} = -\tan(\rho\gamma)\cot(\sigma\gamma), \\ & R = -\tan(\rho\gamma)\cot\left(\left(\frac{\pi}{2} - \rho\right)\gamma\right), \\ & 0 < \gamma < 2, \\ & \max\{0, \pi\gamma - \pi\} \le 2\gamma\rho < \min\{\pi\gamma, \pi\}, \\ & \max\{0, \pi - \pi\gamma\} \le -2\gamma\sigma < \min\{\pi, 2\pi - \pi\gamma\}, \end{aligned}$$

and the solution u belongs to $H^{1+\gamma-\epsilon}$ for any $\epsilon > 0$. This low-regularity problem has been tested, e.g. in [18, Section 5.3] and [16] with parameters

$$\gamma = 0.1, \quad R = \frac{A_1}{A_2} \approx 161.4476387975881, \quad \rho = \frac{\pi}{4}, \quad \sigma \approx -14.92256510455152.$$

In our testing, we set $A_1 = 161.4476387975881$ and $A_2 = 1$.

We test Example 5.3 on the unstructured and successively refined meshes with the initial mesh (see Fig. 5.1) being locally refined near $(0, 0)$, where the exact and numerical solutions exhibit obvious and strong singularity, see Figs. 5.2(a), 5.2(b). This example exactly aligns with our problem setting for the regularity that $u \in H^\gamma, \gamma < 1/2$. Under the setting that the solution $u \in H^{0.1-\epsilon}$ for any arbitrarily small $\epsilon > 0$, we derive the theoretical convergence rates of $\mathcal{O}(h^{0.1})$ in the energy norm and $\mathcal{O}(h^{0.2})$ in the L^2-norm. Notably, these predicted rates hold consistently for both polynomial degrees $k = 1$ and $k = 2$, as evidenced by the numerical data presented in Tables 5.5 and 5.6, where "Mesh level" and "DOFs" are labels for, respectively, successively refined meshes and degree of freedoms. The observed convergence behavior is fundamentally constrained by the limited regularity of the solution u and the regularity of the duality problem, which dominates the error estimates regardless of the polynomial order selected in the discretization. This result aligns with the theoretical framework established in previous sections, highlighting the intrinsic relationship between solution smoothness and convergence rates in numerical approximations.

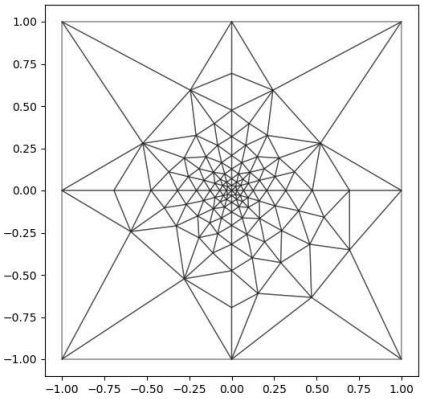

Fig. 5.1. Example 5.3. Initial mesh which is locally refined near the singular point $(0, 0)$.

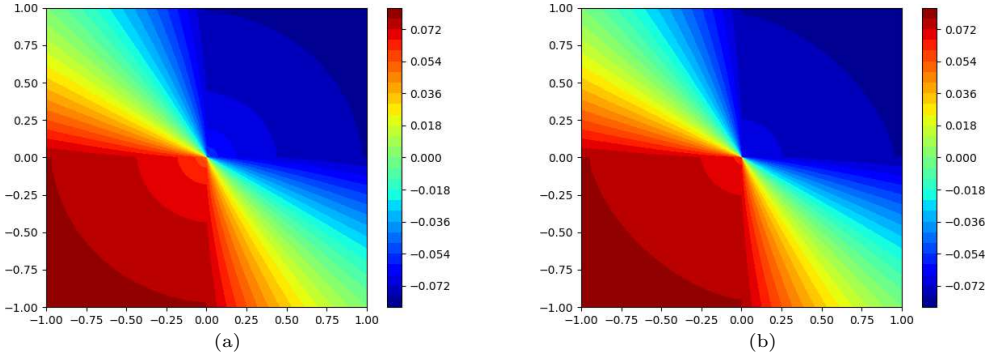

Fig. 5.2. Example 5.3. Plots of u (a) and u_h (b) on the finest mesh.

Table 5.5: Example 5.3. Convergent history of DG ($k = 1, \alpha_F = 3$).

Mesh level	DOFs	$\|u - u_h\|_{V(h)}$	Rate	$\|u - u_h\|_{L^2(\Omega)}$	Rate
1	543	3.0175e-01		4.2901e-03	
2	2172	2.8113e-01	0.1021	3.4799e-03	0.3020
3	8688	2.6831e-01	0.0673	3.0489e-03	0.1908
4	34752	2.5558e-01	0.0701	2.6971e-03	0.1769
5	139008	2.4041e-01	0.0883	2.3943e-03	0.1718

Table 5.6: Example 5.3. Convergent history of DG ($k = 2, \alpha_F = 3$).

Mesh level	DOFs	$\|u - u_h\|_{V(h)}$	Rate	$\|u - u_h\|_{L^2(\Omega)}$	Rate
1	1086	2.8698e-01		1.2264e-03	
2	4344	2.6575e-01	0.1109	9.6012e-04	0.3531
3	17376	2.4765e-01	0.1018	8.1947e-04	0.2285
4	69504	2.3163e-01	0.0965	7.1604e-04	0.1947
5	278016	2.1681e-01	0.0954	6.2798e-04	0.1893

6. Conclusions

In this paper, we have presented a simple proof of IPDG method with lifting operator fluxes. A key ingredient is to use quasi-interpolations satisfying commutative property to establish the numerical error with the oscillation of the right-hand side f. The error estimates are valid for smooth/discontinuous diffusion coefficient and the regularity that $u \in H^{1+s}, 0 \leq s < 1/2$. We also conducted closely related numerical experiments to confirm our findings.

Acknowledgments. The author expresses gratitude to the anonymous referees for their valuable suggestions.

This work is partially supported by National Natural Science Foundation of China (Grant No. 12401549) and by the Yangzhou Innovation Capability Enhancement Fund (Grant No. YZ2024245), China.

References

[1] R.A. Adams and J.J. Fournier, *Sobolev Spaces*, in: *Pure and Applied Mathematics*, Vol. 140, Academic Press, 2003.

[2] D.N. Arnold, F. Brezzi, B. Cockburn, and L.D. Marini, Unified analysis of discontinuous Galerkin methods for elliptic problems, *SIAM J. Numer. Anal.*, **39**:5 (2002), 1749–1779.

[3] A. Bonito, J.L. Guermond, and F. Luddens, Regularity of the Maxwell equations in heterogeneous media and Lipschitz domains, *J. Math. Anal. Appl.*, **408**:2 (2013), 498–512.

[4] S.C. Brenner and L.R. Scott, *The Mathematical Theory of Finite Element Methods*, Springer, 2008.

[5] F. Brezzi, G. Manzini, D. Marini, P. Pietra, and A. Russo, Discontinuous Galerkin approximations for elliptic problems, *Numer. Methods Partial Differential Equations*, **16**:4 (2000), 365–378.

[6] D.A. Di Pietro and A. Ern, *Mathematical Aspects of Discontinuous Galerkin Methods*, in: *Mathématiques et Applications*, Vol. 69, Springer, 2012.

[7] A. Ern and J.L. Guermond, Mollification in strongly Lipschitz domains with application to continuous and discrete de Rham complexes, *Comput. Methods Appl. Math.*, **16**:1 (2016), 51–75.
[8] A. Ern and J.L. Guermond, Finite element quasi-interpolation and best approximation, *ESAIM Math. Model. Numer. Anal.*, **51**:4 (2017), 1367–1385.
[9] A. Ern and J.-L. Guermond, Quasi-optimal nonconforming approximation of elliptic PDEs with contrasted coefficients and $h^{1+r}, r > 0$, regularity, *Found. Comput. Math.*, **22**:5 (2022), 1273–1308.
[10] C. Geuzaine and J.F. Remacle, Gmsh: A 3-D finite element mesh generator with built-in pre- and post-processing facilities, *Int. J. Numer. Methods Eng.*, **79**:11 (2009), 1309–1331.
[11] P. Grisvard, *Elliptic Problems in Nonsmooth Domains*, SIAM, 2011.
[12] T. Gudi, A new error analysis for discontinuous finite element methods for linear elliptic problems, *Math. Comput.*, **79**:272 (2010), 2169–2189.
[13] F. Ihlenburg, *Finite Element Analysis of Acoustic Scattering*, Springer, 1998.
[14] J.D. Joannopoulos, S.G. Johnson, Joshua N. Winn, and R.D. Meade, *Photonic Crystals: Molding the Flow of Light*, Princeton University Press, 2008.
[15] O.A. Karakashian and F. Pascal, A posteriori error estimates for a discontinuous Galerkin approximation of second-order elliptic problems, *SIAM J. Numer. Anal.*, **41**:6 (2003), 2374–2399.
[16] J. Liu, L. Mu, X. Ye, and R. Jari, Convergence of the discontinuous finite volume method for elliptic problems with minimal regularity, *J. Comput. Appl. Math.*, **236**:17 (2012), 4537–4546.
[17] P. Monk, *Finite Element Methods for Maxwell's Equations*, Oxford University Press, 2003.
[18] P. Morin, R.H. Nochetto, and K.G. Siebert, Convergence of adaptive finite element methods, *SIAM Rev.*, **44**:4 (2002), 631–658.
[19] D.A.D. Pietro and A. Ern, Analysis of a discontinuous Galerkin method for heterogeneous diffusion problems with low-regularity solutions, *Numer. Methods Partial Differential Equations*, **28**:4 (2012), 1161–1177.
[20] B. Rivière, *Discontinuous Galerkin Methods for Solving Elliptic and Parabolic Equations*, SIAM, 2008.
[21] L.R. Scott and S. Zhang, Finite element interpolation of nonsmooth functions satisfying boundary conditions, *Math. Comput.*, **54**:190 (1990), 483–493.
[22] L. Tartar, *An Introduction to Sobolev Spaces and Interpolation Spaces*, Springer, 2007.
[23] R. Temam and A. Chorin, *Navier Stokes Equations: Theory and Numerical Analysis*, North-Holland, 1977.
[24] T.P. Wihler and B. Rivière, Discontinuous Galerkin methods for second-order elliptic PDE with low-regularity solutions, *J. Sci. Comput.*, **46**:2 (2011), 151–165.